RSC Advances

PAPER

View Article Online
View Journal | View Issue

Cite this: *RSC Adv.*, 2017, **7**, 37255

Preparation of poly(styrenesulfonic acid) grafted Nafion with a Nafion-initiated atom transfer radical polymerization for proton exchange membranes

Kang-Jen Peng,[a] Juin-Yih Lai[b] and Ying-Ling Liu *[a]

Received 22nd June 2017
Accepted 21st July 2017

DOI: 10.1039/c7ra06984g

rsc.li/rsc-advances

This work reports the synthesis of a poly(styrenesulfonic acid)-grafted Nafion (Nafion-*g*-PSSA) copolymer through atom transfer radical polymerization (ATRP) using Nafion chains as a macroinitiator. The C–F linkages of the –CF– groups and $-CF_2-SO_3H$ groups serve as the initiating sites for the ATRP of the employed styrenic monomer. The PSSA chains further enhance the hydrophilic–hydrophobic microphase separation in the Nafion-*g*-PSSA based membrane, demonstrating relatively large ionic cluster domains and small distances between the hydrophilic and hydrophobic domains compared to the neat Nafion based membrane. Consequently, Nafion-*g*-PSSA is an effective additive for the fabrication of Nafion-based proton exchange membranes. With an optimum fraction of 15 wt% Nafion-*g*-PSSA, the modified Nafion membrane exhibits a proton conductivity of about 97 mS cm^{-1} (95 °C, RH = 100%), which is larger than the values measured on the recast neat Nafion membrane (53 mS cm^{-1}) and a commercial Nafion 212 membrane (88 mS cm^{-1}). The Nafion-initiated ATRP is effective for preparation of Nafion derivative materials for proton exchange membranes.

Introduction

Nafion,[1] a perfluorosulfonic acid polymer, has been widely used as a raw material for the fabrication of polyelectrolyte membranes for electrodialysis[2–4] and proton exchange membranes (PEMs)[5–8] for fuel cells (FCs). The fluorocarbon ether structure of Nafion features good thermal stability and high chemical resistance. Moreover, the beautiful hydrophobic and hydrophilic microphase separation results in the formation of large sulfonic acid domains in the corresponding membranes, so as to contribute to the high proton conductivities of the Nafion-based membranes. On the basis of continuing developments of PEMs having higher proton conductivities than Nafion, nanomaterials have shown some success as effective additives to Nafion that result in Nafion-based nanocomposite membranes[7–13] which exhibit proton conductivities exceeding the values of the pristine recast Nafion membranes and commercial products like Nafion 212. On the other hand, sulfonated hydrocarbon-based polymers and the corresponding polymer blends have been widely studied.[14–17] With sulfonic acid groups locally and densely attached to the polymer chains, some sulfonated hydrocarbon polymers have resulted in membranes showing similar hydrophobic/hydrophilic microphase separations, larger sulfonic acid domains, and high proton conductivities compared to the Nafion-based membranes. For the sulfonated hydrocarbon-based polymers and membranes, the flexible molecular and structural design and chemical synthesis could effectively widen the scope of this class of PEMs for FCs.

The massive studies on the sulfonated hydrocarbon-based PEMs point out that performing chemical reaction on Nafion chains could be a convenient and effective way for designs and synthesis of Nafion-based high performance polyelectrolytes for PEMs. Nevertheless, it is relatively difficult to performance such attempts on Nafion due to the highly chemically stable fluorocarbon ether structure of Nafion chains. Our previous work demonstrated the first chemical reaction on Nafion chains with an ozone-induced oxidation.[11] The ozone treatment generates some hydroperoxide and peroxide groups at Nafion chains. Thermal decomposition of the hydroperoxide/peroxide groups forms free radicals at the Nafion chains to make them becoming chemically reactive toward C=C groups. Based on the reaction route, Nafion chains have been chemically reacted to the outer surfaces of multiwalled carbon nanotubes (MWCNTs),[11] graphene oxide,[6] and maleimide-modified poly(vinylidene difluoride) electrospun nanofibers.[18] The Nafion-modified nanomaterials have been utilized as effective additives for Nafion and other polyelectrolytes to efficiently increase the proton conductivities of the corresponding PEMs.[6,11,18] Nevertheless, the ozone-mediated reaction routes have less flexibility in molecular and structural designs for preparation of Nafion derivatives.

Recently, we have demonstrated that some of the C–F groups of Nafion chains are active groups for atom transfer radical

[a]*Department of Chemical Engineering, National Tsing Hua University, 30013 Hsinchu, Taiwan. E-mail: liuyl@mx.nthu.edu.tw*

[b]*R&D Center for Membrane Technology, Department of Chemical Engineering, Chung Yuan University, Chungli, Taoyuan 32023, Taiwan*

addition and polymerization (ATRA/ATRP) reactions,[19] and the possibility to carry out controllable chemical reactions at Nafion chains. Soon after, Feng *et al.*[20] followed our work and utilized this chemistry of Nafion to prepare poly(vinylimidazole)-grafted Nafion and the corresponding proton exchange membranes with depressed methanol permeability for direct methanol fuel cells. Continuing our efforts on the developments of reactions at Nafion chains and new materials for PEMs, in this work we report the synthesis of poly(styrenesulfonic acid) grafted Nafion (Nafion-PSSA) through ATRP using Nafion as a macroinitiator. The grafted PSSA side chains of the Nafion-*g*-PSSA graft copolymer possess a sulfonic acid group at every repeating unit, so as to increase the density of the sulfonic acid group at the Nafion side chains. While addition of the Nafion-*g*-PSSA graft copolymer to Nafion for fabrication of Nafion-based PEMs, the Nafion portion of Nafion-*g*-PSSA serves as a compatilizer to the Nafion matrix, and the PSSA portion contributes to induce the aggregation of sulfonic acid groups so as to result in an increase in the hydrophilic domain sizes of the resulting PEMs. As a result, the Nafion-*g*-PSSA modified Nafion membrane shows a proton conductivity of about 97 mS cm^{-1} (95 °C, RH = 100%), compared to the values of 53 and 88 mS cm^{-1} recorded on the recast neat Nafion membrane and commercial Nafion 212 membrane, respectively.

Experimental

Materials

A commercial product of Nafion dispersion (D2020, 20 wt% of Nafion with an acid capacity of about 1.00 meq g^{-1}) was used as received. Sodium styrene sulfonate (NaSS) was purchased from Aldrich Chemical Co. 2,2′-Dipyridine (>99%) and copper(I) bromide (CuBr) (98%) were purchased from Acros Organics Co. Reagent grade solvents and distilled water were used as solvents without further purification.

Instrumental methods

Fourier transform infrared (FTIR) spectra were recorded with a Perkin Elmer Spectrum 2 FTIR instrument. Solid samples were grounded with dry KBr powder and pelleted for measurements taken in the wavenumber range of 400–4000 cm^{-1}. ^{19}F nuclear magnetic resonance (NMR) measurements were taken with a Brüker AVANCE 500 NMR Spectrometer (500 MHz). Thermogravimetric analysis was conducted with a Thermal Analysis TA-Q500 TGA instrument under a nitrogen flow (100 mL min^{-1}) at a heating rate of 10 °C min^{-1}. X-ray photoelectron spectroscopic analysis (XPS) was performed with an XPS instrument of Model Sigma Probe provided with Thermo VG-Scientific Company. A Mg-K_α R-ray radiation line is used as the incident beam. Mechanical properties of PEMs were measured with an instron machine (Instron 5543 Analyzer) with an elongation rate of 5 mm min^{-1}. The samples were dried under vacuum at room temperatures prior to measurements. Atomic force microscopy (AFM) measurements were recorded with a scanning probe microscope system of Brüker Dimension Icon instrument. The AFM tip holder for liquid phase is DECAFMCH-DD and the AppNano HYDRA-ALL series AFM tip is used with a spring constant of 0.3 N m^{-1}. Peak force tapping mode for liquid phase and general tapping mode were taken for for the images shown in Fig. 4 and 6, respectively. Small angle X-ray scattering (SAXS) measurements were conducted with a Brüker Nanostar SAXS machine with a radiation beam in the wavelength of 0.1541 nm. The utilized instrument is equipped with a 2D position-sensitive detector of Brüker AXS.

Measurements of proton conductivities

The proton conductivities of the prepared membranes were performed with the method reported previously.[18] The membranes were hydrated with deionic water at room temperature (about 25 °C) for 24 h prior to measurements. The hydrated membrane was applied to the measurement with a 4-point-probe method in a fully hydrated chamber with a 100% relative humidity. The membrane was clamped between two electrodes (effective area: 1.0 cm^2). The membrane resistances was measured with a frequency response analyzer (Solartron 1255B) equipped with a Solartron SI 1287 electrochemical interface at an oscillation amplitude of 10 mV and a frequency range of 10^2 to 10^6 Hz at a desired temperature. Proton conductivities of the membranes at various temperatures were recorded.

Preparation of the graft copolymer of Nafion

NaSS (2.06 g, 10 mmol) was dissolved in in a mixture of water and isopropanol (IPA) (10 mL, IPA/water = 2/1 v/v). The solution was then added to the D2020 Nafion suspension (6.0 g). After addition of 2,2′-bipyridyl (0.062 g, 0.4 mmol) and CuBr (0.01 g, 0.07 mmol), the reaction solution was purged with an argon stream for 15 min. and degassed twice with the freeze–pump–thaw process. The solution was reacted at room temperature for 24 h and drop into excess water. The precipitant was collected with centrifugation and purified with the solution-precipitation process twice. Finally, the collected sample was washed with water and dried under vacuum at room temperature to give the product of Nafion-*g*-PNaSS (0.45 g).

Fabrication of Nafion based membranes

A certain amount of Nafion-PNass was added to the D2020 Nafion solution (1 g). After standing at room temperature for 12 h, the solution was cast on a glass plate, dried at 50 °C for 1 h and 80 °C for 1 h. The peeling-off Nafion-based membrane was treated with 1 N sulfuric acid solution at 80 °C (converting the sodium sulfonate of PNaSS to be sulfonic acid), washed with water at 80 °C, and finally dried at 80 °C under vacuum. The modified Nafion-based membranes were coded as M-Nafion-*X*, where *X* denotes to the weight fractions of Nafion-PNaSS in the membranes. Four M-Nafion-*X* membranes with an *X* value of 5, 10, 15, and 20 have been prepared in this work.

Results and discussion

Preparation of poly(sodium styrenesulfonate) grafted Nafion copolymer

Graft of poly(sodium styrene sulfonate) (PNaSS) chains to Nafion has been carried out with ATRP of using NaSS as

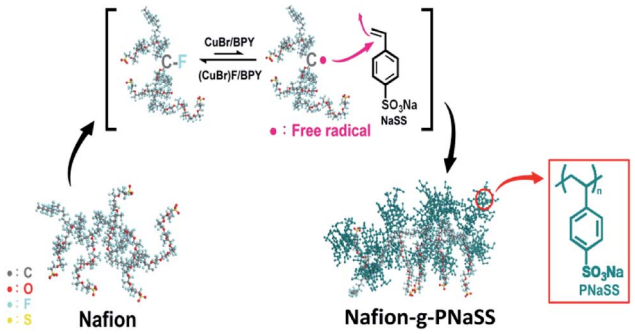

Fig. 1 Preparation of PNaSS grafted Nafion copolymer with ATRP using Nafion as a macro-initiator.

a monomer, Nafion as a macroinitiator, CuBr as a catalyst, and 2,2′-bipyridyl as a ligand (Fig. 1).[19] The reactive sites of Nafion chains responsible for initiating ATRP of NaSS have been verified with ^{19}F NMR measurements on the reaction system. As shown in Fig. 2, the signal intensity of peaks b and g decreases obviously to indicate that the C–F groups of –CF–O– at the main chains and $–CF_2–SO_3H$ at the side segments of Nafion involve in the ATRP of NaSS as initiating sites. Moreover, according to the previous work the –C–F groups of $–CF(CF_3)–O–$ (peak d) at the side segments might also be potential initiating sites for ATRP. Nevertheless, the reaction of $–CF_2–SO_3H$ would convert some $–CF_2–$ groups to be –CFC– groups which contribute to increase the signal intensity of peaks d in the ^{19}F NMR spectrum of Nafion-*g*-PSSA. The potential initiating sites for the Nafion chains are the –C–F linkages of b, d, and g shown in Fig. 2. All the results show good coincidence to that reported in our previous paper.[19]

The spectral characterization of Nafion-*g*-PNaSS has been collected in Fig. 3. For the FTIR spectrum of Nafion-*g*-PNaSS, the absorption of aromatic rings at about 1500 and 1600 cm^{-1} and the absorption of $Ph–SO_3–$ at about 1011 cm^{-1} supports to the incorporation of PNaSS chains to Nafion. In addition, the characteristic absorption corresponding to Nafion structure includes $–CF_2–$ at 1240 and 1150 cm^{-1}, $–SO_3$ at 1060 cm^{-1}, –C–F at 980 cm^{-1}, and C–O–C at 973 cm^{-1}. Similar results have been also obtained with the C_{1s} core-level XPS analysis on Nafion-PNaSS. In addition to the characteristic peaks of contributed from Nafion chains ($–CF_3$ at 293.3 eV, $–CF_2–$ at 291.9 eV, –CF– at 291.1 eV, and $CF–SO_3H$ at 289.4 eV), the presence of PNaSS chains could be characterized with the peaks of $C–SO_3H$ at 286.3 eV, C–C at 285.0 eV, and C–H at 284.6 eV. As the neat Nafion sample does not show these peaks in the XPS spectrum, the results provide strong supports to the successful preparation of the Nafion-*g*-PNaSS graft copolymers. The neat Nafion gives an F/C ratio of about 1.45 in XPS analysis. After grafts of PNaSS chains, the Nafion-*g*-PNaSS shows a decreased F/C ratio of about 1.13. The introduction of PNaSS segments also results in an increase in the S content of the graft copolymer, as the F/S ratio decrease from 30.4 (measured with Nafion) to 17.8 (measured with Nafion-*g*-PNaSS). Based on the F/C ratios, the weight fraction of PNaSS segments of the Nafion-*g*-PNaSS graft copolymer is about 15.6 wt%.

The samples have also been applied to TGA measurements. The weight loss at about 300 °C observed with the pristine Nafion could be attributed to the degradation of the sulfonic

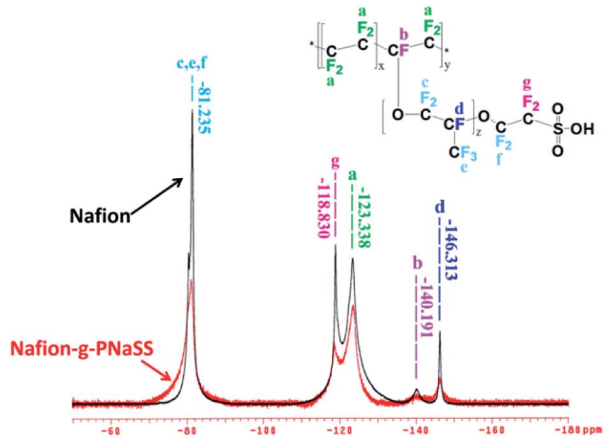

Fig. 2 ^{19}F NMR spectra of Nafion and Nafion-*g*-PNaSS copolymer supporting to the active species of Nafion chains in ATRP reaction.

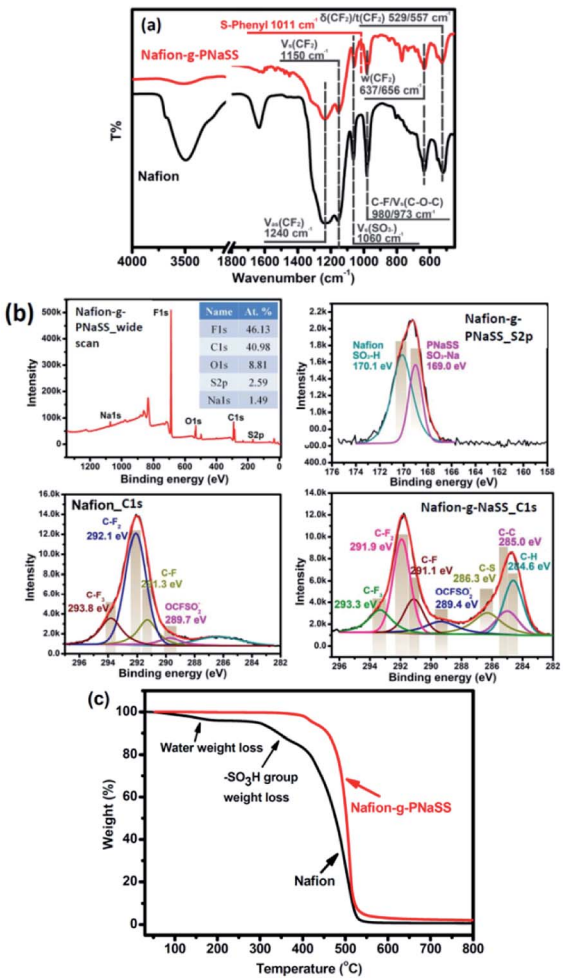

Fig. 3 (a) FTIR, (b) XPS, and (c) TGA measurements on Nafion-*g*-PNaSS copolymer.

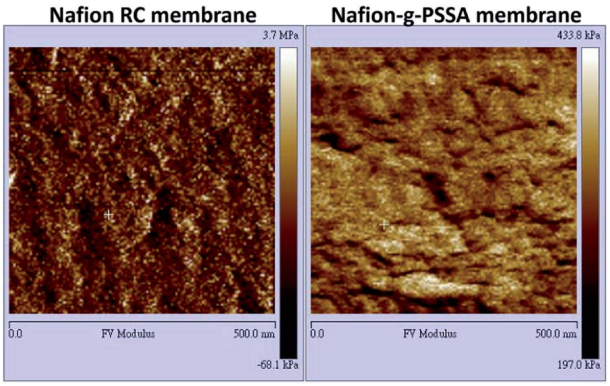

Fig. 4 AFM micrographs of Nafion RC membrane and Nafion-*g*-PSSA based membrane.

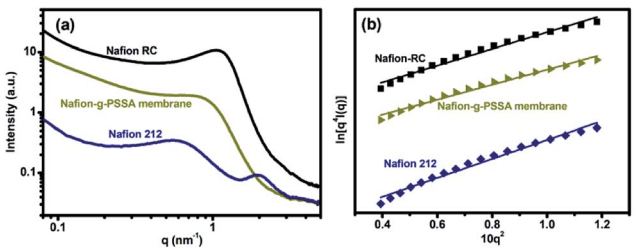

Fig. 5 (a) SAXS spectra and (b) the corresponding Porod plots measured on Nafion RC, Nafion 212, and Nafion-*g*-PSSA based membrane.

acid groups.[21] After introduction of PNaSS chains to the Nafion backbone, the thermal stability of the sulfonic groups of Nafion chains increases due to the interaction between the sulfonic acid groups and the sulfonate groups of PNaSS chains. Nevertheless, the major weight losses of the two polymers occur at different temperatures. The relatively high degradation temperature of Nafion-*g*-PNaSS could be attributed to the high thermal stability of PNaSS chains. Moreover, the thermal stability of the sulfonic acid groups of Nafion has been enhanced with their strong interaction with the sulfonate groups of PNaSS. A similar result is discussed in the literature.[21]

The above characterization supports to the successful preparation of Nafion-*g*-PNaSS graft copolymer through ATRP using Nafion as a macroinitiator. Consequently, Nafion-*g*-PNaSS has been fabricated into a dense membrane with a conventional solution casting method. Treatment of the Nafion-*g*-PNaSS membrane transforms the corresponding membrane in acid form (poly(styrene sulfonic acid)-grafted Nafion (Nafion-*g*-PSSA) membrane). The transformation has been verified with the disappearance of Na signal in XPS wide-scan measurements. Under an AFM observation (Fig. 4), the hydrophilic and hydrophobic microphase separation shows contrast dark (relatively soft hydrophilic sulfonic groups) and bright (relatively rigid hydrophobic chains) regions.[22,23] The Nafion-*g*-PSSA membrane shows a clear hydrophilic–hydrophobic microphase separation with a large hydrophilic domain size, compared to the neat recast Nafion membrane. This result implies the formation of proton-transportation channels in the Nafion-*g*-PSSA membrane. The enhanced microphase separation of the Nafion-*g*-PSSA membrane has further been examined with SAXS measurements (Fig. 5). The commercial product of Nafion 212 shows a scattering peaks at q value of about 0.55 and 1.97 nm^{-1} corresponding to its crystalline size and domain size of sulfonic acid clusters, respectively.[24] Compared to Nafion-RC membrane which shows a scattering peak at q value of about 1.06 nm^{-1}, the q value recorded with the Nafion-*g*-PSSA membrane is about 0.78 nm^{-1}. The small q value of the Nafion-*g*-PSSA membrane indicates that it possesses relatively large domain sizes of ionic clusters.[25,26] On the other hand, the other peak observed with Nafion 212, which corresponds to the regularity of crystalline structure, is not discernable for the Nafion-RC and Nafion-*g*-PSSA membranes, as poor crystailline structures of the casted Nafion membranes.[27] The slopes read from the Porod plots (plots of $\ln[q^4I(q)]$ *vs.* $10q^2$), which reveal the information about the distance between the hydrophilic and hydrophobic domains,[28–30] still gives a similar result. The value of the Porod plot slope measured on Nafion-RC and Nafion-*g*-PSSA is about 2.46 and 2.22 nm^2, respectively. The Nafion-*g*-PSSA membrane possesses a short distance between hydrophilic and hydrophobic domains, so as to provide a promoted pathway for ion transportation through the membrane. All the results suggest that graft of PSSA segments to Nafion chains could enhance the proton conductivity of the corresponding membrane. Nevertheless, the Nafion-*g*-PSSA membrane exhibits a high water-uptake of about 80% and poor dimensional stability in an aqueous environment. Further examination on the Nafion-*g*-PSSA membrane for PEMs does not give reliable results.

Table 1 Properties of the Nafion-based membranes studied in this work

Membrane	Water uptake (wt%)	*X–Y* dimensional change for fully hydrated sample (%)	Mechanical properties			Proton conductivity (mS cm^{-1})	
			Young's modulus (MPa)	Stress at break (MPa)	Elongation at break (%)	20 °C	95 °C
Nafion-RC	44 ± 4	27 ± 3	123 ± 42	21.0 ± 2.4	268 ± 44	26	53
M-Nafion-5	50 ± 4	29 ± 6	145 ± 55	17.0 ± 4.0	258 ± 49	44	83
M-Nafion-10	54 ± 4	35 ± 10	143 ± 80	18.5 ± 2.4	280 ± 66	50	83
M-Nafion-15	54 ± 6	42 ± 8	138 ± 67	18.4 ± 1.6	298 ± 45	57	97
M-Nafion-20	67 ± 7	50 ± 14	120 ± 45	18.8 ± 0.8	323 ± 28	38	66

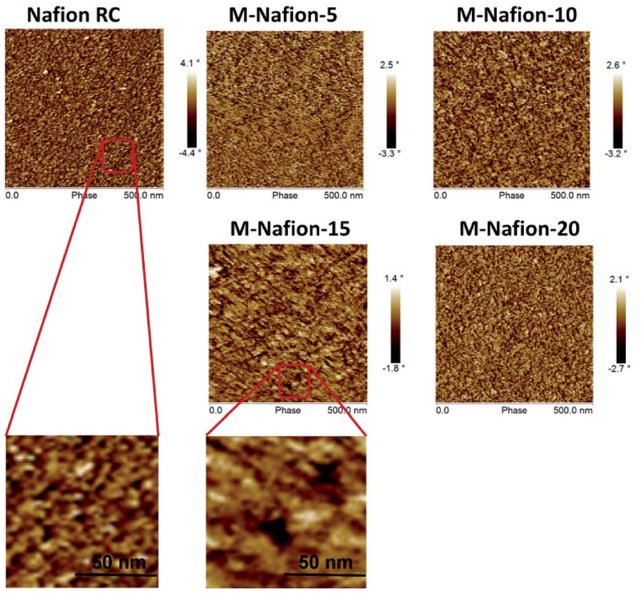

Fig. 6 AFM micrographs of Nafion RC membrane and the Nafion based membranes modified with various amounts of Nafion-*g*-PSSA copolymer.

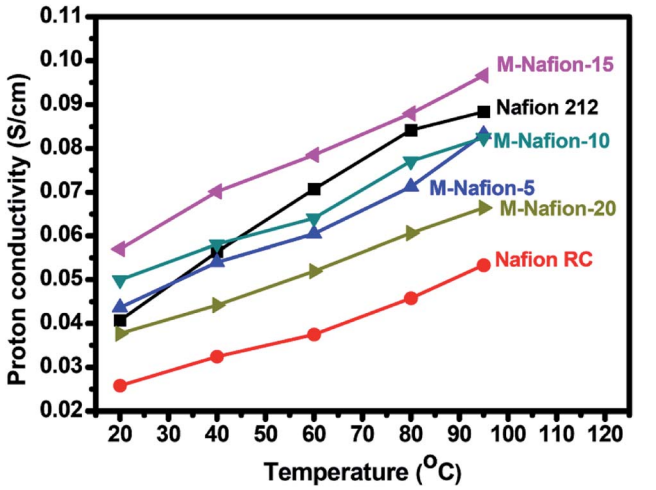

Fig. 7 Temperature-dependent proton conductivities of the Nafion based membranes studied in this work.

Fabrication and properties of Nafion-*g*-PSSA-modified Nafion based membranes

Nafion-*g*-PNaSS is then utilized as a modifier for Nafion for fabrication of modified Nafion-based membranes. The measured properties of the Nafion-based membranes are collected in Table 1. The water uptakes and *X*–*Y* dimensional changes both increase with increasing the amounts of Nafion-*g*-PSSA in the membranes. The dimensional stability of M-Nafion-20 is relatively poor due to its high Nafion-*g*-PSSA content. On the other hand, addition of Nafion-*g*-PSSA to the Nafion-based membranes does not alter their mechanical properties obviously. All the membranes in dry states exhibit similar mechanical strength and toughness. The hydrated membranes were failure for mechanical tests. The mechanical properties of the Nafion-based membranes warrant their suitability for application in PEMFCs.

Fig. 6 shows the AFM images of the Nafion-based membranes in wet state. The hydrophilic ion clusters become obvious for the Nafion-*g*-PSSA modified membranes. As labled in Fig. 6, the hydrophilic domain size of Nafion-RC membrane is about 6 nm. With addition of 15 wt% of Nafion-*g*-PSSA, a large domain size of about 16 nm is observed with the M-Nafion-15 membrane. The result suggests that the long PSSA chains of Nafion-*g*-PSSA might enhance the extent of phase separation between the hydrophilic and hydrophobic domains of the Nafion membranes, so as to increase the sizes of the proton-conductive channels in the Nafion membrane.[16,17] Nevertheless, the M-Nafion-20 membrane shows a relatively small domain size compared that of M-Nafion-15.

The neat recast Nafion membrane (Nafion-RC) shows a proton conductivity of 26 and 53 mS cm^{-2} at 20 and 95 °C, respectively (Table 1 and Fig. 7). Addition of 15 wt% of Nafion-*g*-PSSA to the Nafion membrane significantly increases the proton conductivity of the resulting membrane (M-Nafion-15), as M-Nafion-15 shows a proton conductivity of 57 and 97 mS cm^{-2} at 20 and 95 °C, respectively. The enhanced proton conductivity could be attributed to the increased sizes of hydrophilic domains forming ion-transportation channels in the membrane. Similarly, the proton conductivity of M-Nafion-20 is not as high as that of M-Nafion-15. The results support to the application of Nafion-*g*-PSSA for fabrication of high performance PEMs for fuel cells.[20]

Conclusion

Nafion-initiated ATRP is an effective reaction approach to synthesize Nafion derivatives. Nafion-*g*-PSSA graft copolymer has been successfully prepared and characterized. Introduction of PSSA chains to Nafion derivative promotes the hydrophilic–hydrophobic microphase separation in the corresponding membrane, consequently demonstrating enlarged ionic cluster domains and shortened distance between the hydrophilic and hydrophobic domains. Effective proton conducting channels forms in the membrane. Therefore, utilization of the Nafion-*g*-PSSA graft copolymer as an additive for Nafion could increase the proton conductivities of the resulting Nafion-based membranes, and enhance their potential of applications in proton exchange membranes and other fields. Reaction of Nafion chains could extend the windows of structural designs and properties of Nafion based materials.

Acknowledgements

The authors thank the Ministry of Science and Technology (MOST) of Taiwan (Grant No. MOST 105-2221-E-007-138-MY3) for the financial supports on this work. KJP acknowledges the postdoctoral researcher fellowship supported with MOST of Taiwan and Chang Chun Plastics Company (MOST 105-2622-8-007-009).

References

1 K. A. Mauritz and R. B. Moore, *Chem. Rev.*, 2004, **104**, 4535–4586.
2 N. White, M. Misovich, A. Yaroshchuk and M. L. Bruening, *ACS Appl. Mater. Interfaces*, 2015, **7**, 6620–6628.
3 N. White, M. Misovich, E. Alemayehu, A. Yaroshchuk and M. L. Bruening, *Polymer*, 2016, **103**, 478–485.
4 T. C. Tsai, C. W. Liu and R. J. Yang, *Micromachines*, 2016, **7**, 205 (9 pages).
5 K. Schmidt-Rohr and Q. Chen, *Nat. Mater.*, 2008, **7**, 75–83.
6 K. J. Peng, J. Y. Lai and Y. L. Liu, *J. Membr. Sci.*, 2016, **514**, 86–94.
7 H. Wang, X. Li, X. Zhuang, B. Cheng, W. Wang, W. Kang, L. Shi and H. Li, *J. Power Sources*, 2017, **340**, 201–209.
8 W. Jia, B. Tang and P. Wu, *ACS Appl. Mater. Interfaces*, 2017, **9**, 14791–14800.
9 I. Nicotera, C. Simari, L. Coppola, P. Zygouri, D. Gournis, S. Brutti, F. D. Minuto, A. S. Aricò, D. Sebastian and V. Baglio, *J. Phys. Chem. C*, 2014, **118**, 24357–24368.
10 R. Kannan, B. A. Kakade and V. K. Pillai, *Angew. Chem., Int. Ed.*, 2008, **47**, 2653–2656.
11 Y. L. Liu, Y. H. Su, C. M. Chang, S. Suryani, D. M. Wang and J. Y. Lai, *J. Mater. Chem.*, 2010, **20**, 4409–4416.
12 L. G. Boutsika, A. Enotiadis, I. Nicotera, C. Simari, G. Charalambopoulou, E. P. Giannelis and T. Steriotis, *Int. J. Hydrogen Energy*, 2016, **41**, 22406–22414.
13 E. Bakangura, L. Wu, L. Ge, Z. Yang and T. Xu, *Prog. Polym. Sci.*, 2016, **57**, 103–152.
14 J. Rozière and D. J. Jones, *Annu. Rev. Mater. Res.*, 2003, **33**, 503–555.
15 M. A. Hickner, H. Ghassemi, Y. S. Kim, B. R. Einsla and J. E. McGrath, *Chem. Rev.*, 2004, **104**, 4587–4612.
16 Y. L. Liu, *Polym. Chem.*, 2012, **3**, 1373–1383.
17 Y. Hu, X. Li, L. Yan and B. Yue, *Fuel Cells*, 2017, **17**, 3–17.
18 H. Y. Li and Y. L. Liu, *J. Mater. Chem. A*, 2014, **2**, 3783–3793.
19 K. J. Peng, K. H. Wang, K. Y. Hsu and Y. L. Liu, *ACS Macro Lett.*, 2015, **4**, 197–201.
20 K. Feng, L. Liu, B. Tang, N. Li and P. Wu, *ACS Appl. Mater. Interfaces*, 2016, **8**, 11516–11525.
21 Q. Deng, C. A. Wilkie, R. B. Moore and K. A. Mauritz, *Polymer*, 1998, **39**, 5961–5972.
22 N. Li, D. S. Hwang, S. Y. Lee, Y. L. Liu, Y. M. Lee and M. D. Guiver, *Macromolecules*, 2011, **44**, 4901–4910.
23 P. J. James, J. A. Elliott, T. J. McMaster, J. M. Newton, A. M. S. Elliott, S. Hanna and M. J. Miles, *J. Mater. Sci.*, 2000, **35**, 5111–5119.
24 F. M. Collette, F. Thominette, H. Mendil-Jakani and G. Gebel, *J. Membr. Sci.*, 2013, **435**, 242–252.
25 H.-G. Haubold, T. Vad, H. Jungbluth and P. Hiller, *Electrochim. Acta*, 2001, **46**, 1559–1563.
26 T. Mochizuki, K. Kakinuma, M. Uchida, S. Deki, M. Watanabe and K. Miyatake, *ChemSusChem*, 2014, **7**, 729–733.
27 J. Lu, H. Tang, C. Xu and S. P. Jiang, *J. Mater. Chem.*, 2012, **22**, 5810–5819.
28 Z. S. Mo and H. F. Zhang, *Structure of crystalline polymers by X-ray diffraction*, Science Publishing Company, China, 2003, pp. 307–311.
29 A. Saccà, A. Carbone, R. Pedicini, G. Portale, L. D'Ilario, A. Longo, A. Martorana and E. Passalacquaa, *J. Membr. Sci.*, 2006, **278**, 105–113.
30 C. M. Chang, H. Y. Li, J. Y. Lai and Y. L. Liu, *RSC Adv.*, 2013, **3**, 12895–12904.

